Fluid Phase Equilibria 425 (2016) 342–350

Contents lists available at ScienceDirect

Fluid Phase Equilibria

journal homepage: www.elsevier.com/locate/fluid

Polyether polyol/CO_2 solutions: Solubility, mutual diffusivity, specific volume and interfacial tension by coupled gravimetry-Axisymmetric Drop Shape Analysis

Maria Rosaria Di Caprio [a], Giovanni Dal Poggetto [b], Maria Giovanna Pastore Carbone [a, c], Ernesto Di Maio [a, *], Sara Cavalca [d], Vanni Parenti [d], Salvatore Iannace [e]

[a] Dipartimento di Ingegneria Chimica, dei Materiali e della Produzione Industriale, University of Naples Federico II, P.le Tecchio 80, 80125 Naples, Italy
[b] Institute for Polymers, Composites and Biomaterials, National Research Council, Via Campi Flegrei 34, 80078 Pozzuoli, Naples, Italy
[c] Institute of Chemical Engineering Sciences, Foundation of Research and Technology-Hellas (FORTH/ICE-HT), Stadiou Street, Platani, Patras Achaias 26504, Greece
[d] Dow Italia s.r.l, Polyurethanes R&D, Via Carpi 29, 42015 Correggio, Italy
[e] Institute for Macromolecular Studies, National Research Council, Via Edoardo Bassini, 15, 20133 Milan, Italy

ARTICLE INFO

Article history:
Received 29 March 2016
Received in revised form
8 June 2016
Accepted 9 June 2016
Available online 14 June 2016

Keywords:
Polyol
CO_2
Solubility
Diffusivity
Interfacial tension
Specific volume

ABSTRACT

In this work we investigate the sorption of CO_2 in a formulated polyether polyol, typically used to obtain rigid polyurethane foams when it reacts with isocyanates. In particular, by using a fully-experimental, coupled gravimetry-Axisymmetric Drop Shape Analysis, solubility, mutual diffusivity, specific volume and interfacial tension of polyol/CO_2 solutions have been measured at 35 °C and at CO_2 pressures up to 8000 kPa.

CO_2-treated polyol was also subjected to Gel Permeation Chromatography (GPC) and Fourier Transform Infrared (FT-IR) spectroscopic analysis to evaluate the effect of the high-CO_2 pressure treatment. The results show quite a large CO_2 solubilization (up to 17% ca. in the examined experimental range), in turn responsible for a moderate swelling of the polymer and an extensive effect on the interfacial tension, which reaches vanishing values at the highest investigated pressure.

© 2016 Elsevier B.V. All rights reserved.

1. Introduction

Rigid polyurethane foams (PURs) are closed-cell foamed plastic materials with excellent thermal insulating properties, used as a factory made material in the form of insulation boards or blocks, or in combination with various rigid facings for appliances as a construction material. In addition to the low thermal conductivity, PURs are stable and durable, which is an important feature to guarantee the stability of the insulating properties. In fact, in building applications, these materials must work for as long as the building stands and should have a useful life beyond 50 years [1].

The thermal insulation properties of PURs are due to the presence of closed micro-cells, filled with inert gases, which work, at micron scale, as insulated glazing do at macroscopic scale in reducing heat transfer in buildings. Thermal conductivities, depending on the total gas content (void volume fraction), on the pore topology (foam morphology) and on the thermal conductivities of both the polymer matrix and the gas [2], may reach values as low as 12 mW/(m K) [1]. Until recently, the inert gas most commonly used in polyurethane foams was R-11 (trichlorofluoromethane, CFC-11). However, the Montreal Protocol on substances that deplete the ozone layer has called for the phasing out of the use of CFCs and their replacement with hydrocarbons, hydrofluorocarbons and CO_2. In particular, CO_2 is environmentally friendly and offers a long-term sustainable solution, due to its zero Ozone Depletion Potential (ODP) and its lowest Global Warming Potential (GWP), set equal to 1 as reference to other Green-House-Gases (GHG). Furthermore, CO_2 is non-flammable and is inexpensive, as it is readily available in the atmosphere and other natural sources [1].

The foamed structure of PURs is obtained by the simultaneous gelation reaction between polymeric precursors (polyol and

* Corresponding author.
E-mail address: edimaio@unina.it (E. Di Maio).

http://dx.doi.org/10.1016/j.fluid.2016.06.023
0378-3812/© 2016 Elsevier B.V. All rights reserved.

isocyanate) and gas generation, which can result from a physical, chemical or mechanical process. In physical foaming, a fluid such as hydrocarbons (mainly cyclopentane), hydrofluorocarbons or CO_2, is first solubilized at high pressure in the polymeric precursors at ambient temperature and then it is allowed to evolve from the solution by pressure quench (in this case, no chemical reaction involves the blowing process and the fluid is called Physical Blowing Agent (PBA)). In chemical foaming, the blowing agent is generated from a chemical reaction. Typically, the addition of water in the formulation allows for the reaction of water with isocyanate, to give unstable carbamic acid that decomposes to amine and CO_2 as a by-product, which blows the polymer [2]. In mechanical foaming, the gas, most commonly air, is dispersed into the starting components by vigorous agitation, which leaves entrapped air bubbles within the polymeric matrix. Most commonly, both PBA and water are used, in a combined chemical and physical foaming manner, with CO_2 being present in the reaction media in a dual form, as resulting from the chemical reaction of water with isocyanate and as a physical blowing agent, solubilized under pressure in either the polyol or the isocyanate component. The addition of water has to be finely controlled, as its reaction with the isocyanate may give polyurea as a by-product, which has detrimental effects on some physical and mechanical properties of the final foamed products, such as the stiffness and the strength, and has negative effects on processability [3].

In this context, it is of great importance to know how CO_2 gets into the polymeric precursors, to design the process and the equipment and to optimize the foaming reaction. For instance, CO_2 solubility will determine the amount of gas available for blowing the polymer, in turn defining the final density of the foam, while diffusivity determines the minimal residence time of contact between the gas and the polymeric precursors at processing temperature and pressure to achieve the desired polymer/gas solution. In foaming, furthermore, it has been evidenced how low molecular weight penetrants (in our case, CO_2) extensively affect other properties of the polymer/penetrant solutions, which are involved in the foaming process, namely the interfacial tension of the polymer/penetrant solution in contact with the penetrant and, to a lesser extent, the specific volume of the polymer/penetrant solutions.

A number of experimental techniques are available to measure the aforementioned properties of polymer/gas solution at processing pressures and temperatures; for a review on these techniques, the reader may refer to Di Maio et al. [4]. In this context, recently, Pastore Carbone et al. [5] introduced a coupled sorption-Axisymmetric Drop Shape Analysis (ADSA) technique to simultaneously measure the solubility, diffusivity, interfacial tension and specific volume of polymer/gas solutions in a single experiment. The coupling between gravimetric and optical measurements allows for a fully experimental determination of the aforementioned properties, without resorting to any predictive modeling, as is typically done to evaluate the specific volume of the polymer/gas solution which is needed to calculate sorbed amount and interfacial tension.

To the best of our knowledge, only two papers addressed sorption of CO_2 in polyols. Kazarian et al. [6] simultaneously measured CO_2 sorption and swelling in polyether polyols such as polyethylene glycol (PEG) and polypropylene glycol (PPG) by using in-situ near-infrared spectroscopy. Authors reported data on CO_2 sorption in PEG and corresponding volume increase (swelling) at 40 °C and up to 11600 kPa, evidencing a solubility of CO_2 of 22.6% by weight and a swelling of 35%; for PPG, measurement have been conducted at 25 °C and 35 °C and at pressures up to 6000 kPa. In particular, at 35 °C and 6000 kPa authors observed a solubility of 11.8% by weight and a swelling of 24.5%. Fieback et al. [7] measured the sorption of CO_2 and N_2 in a formulation of polyol (without any further details on its chemistry) and the correspondent swelling by using a magnetic suspension balance equipped with a view cell. Sorption experiments were conducted at temperatures ranging from 20 °C to 40 °C and at pressures up to 6000 kPa, and revealed a maximum in solubility of 38.2% by weight and a swelling as high as 47% at 20 °C and at 5400 kPa. To the best of our knowledge, no data have been reported so far on polyol/CO_2 mutual diffusivity and interfacial tension.

In this work, we report the use of the recently developed equipment based on the coupled sorption-ADSA [5,8] to measure solubility, mutual diffusivity, specific volume and interfacial tension of polyol/CO_2 solution. Measurements have been performed at 35 °C and at CO_2 pressures up to 6800 kPa.

2. Experimental section

2.1. Experimental set-up

The direct and simultaneous determination of solubility, diffusivity, interfacial tension and specific volume of polyol/CO_2 solutions is based on the coupling of gravimetric measurement with ADSA. In detail, it consists in the combination of the gravimetric determination of mass transfer from the CO_2 phase to the polyol contained in a crucible, and the simultaneous optical observation of volume and shape changes of a pendant drop (see Fig. 1). The adopted experimental set-up, schematized in Fig. 2, consists of a magnetic suspension balance (MSB) (Rubotherm Prazisionsmesstechnik GmbH, Germany) equipped with a high pressure and temperature (HT-HP, up to 250 °C and 13500 kPa) view cell, where a custom-designed cylindrical crucible containing 0.5 g ca. of polyol hangs from the hook of the balance weight measuring assembly, and a rod is fixed inside the cell to which the polyol pendant drop is attached. In this experimental configuration, the balance is continuously measuring the weight change of the polyol contained in the crucible and, at the same time, a high-resolution digital camera acquires the profile of the pendant drop. The relative position of the crucible and of the rod is such to avoid any interference with the gravimetric measurement and to allow the reliable continuous acquisition of the drop shape. Drop changes in volume and shape were observed through two optical quality windows, by using an adjustable high resolution CCD camera (BV-7105H, Appro), equipped with a modular zoom lens system (Zoom6000, Navitar). The CCD camera is connected to a computer, and a commercial software (FTA32 Video 2.0, First Ten Angstroms) is used to analyze drop profile [5,8]. Furthermore, in order to achieving the optimal threshold background for digitizing the drop image, a uniform bright background was provided by light emitting diodes. Detailed description of the equipment and of some preliminary experimental phases, such as optimization of CCD parameters and image calibration (pixel/μm calibration and aberration correction), are described elsewhere [5].

The data flow adopted for the elaboration of the data acquired during the coupled sorption-ADSA measurement is illustrated in Fig. 3. First, from the gravimetric experiment, apparent solubility (i.e. not yet corrected to account for the effect of change of sample buoyancy due to sorption and compressive action of pressure) was measured as a function of gas pressure. Concurrently, from ADSA, the profile of the pendant polyol/gas drop was computed. As described in detail in Pastore Carbone et al. [5], data from ADSA were used to evaluate the volume of the polyol/CO_2 solution contained in the crucible (A), thus allowing for the correction of sorption data with the proper buoyancy force and, consequently, for the calculation of actual solubility and diffusivity of the polyol/CO_2 solution at each gas pressure (B). Then, the specific volume of

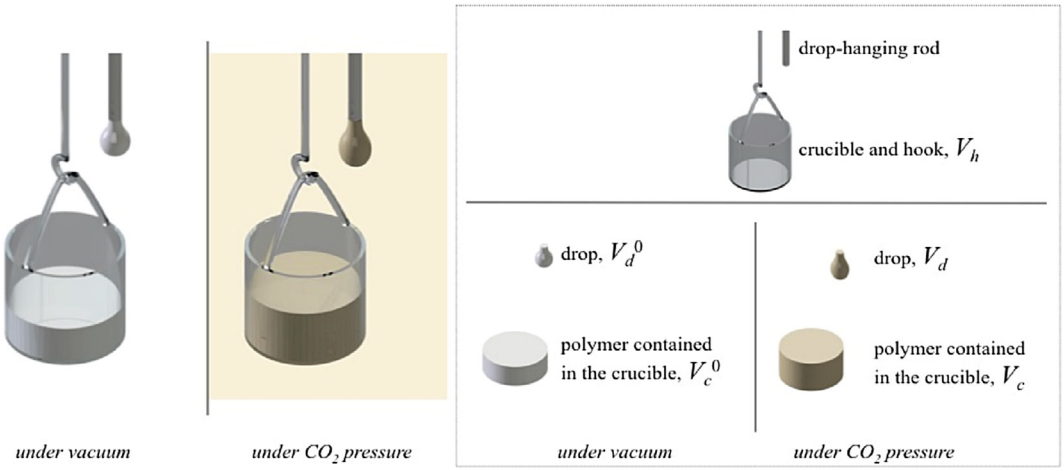

Fig. 1. Schematization of the samples and sample holders and definitions of the volumes addressed to in the text, under vacuum or under any CO_2 pressure.

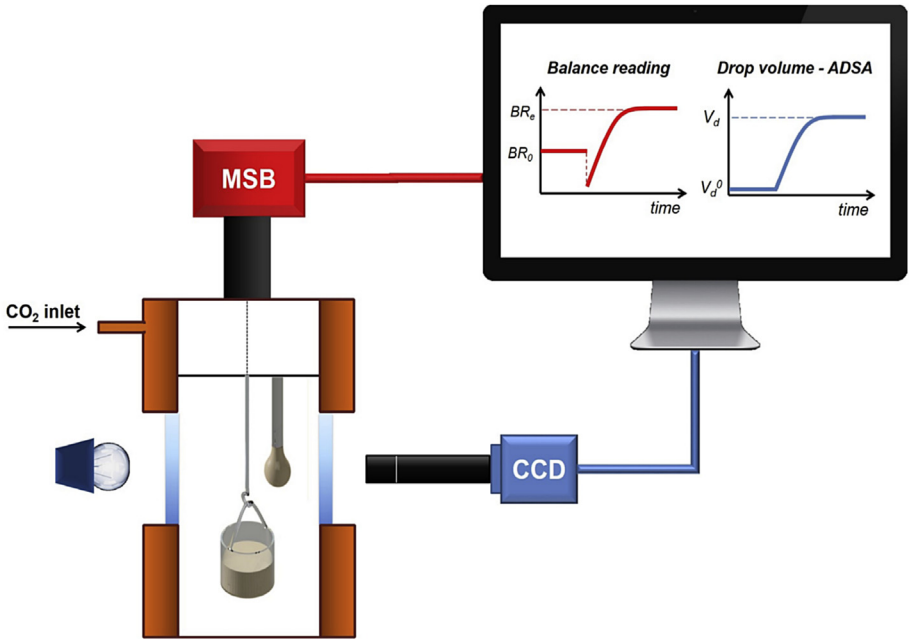

Fig. 2. Schematic illustration of the experiment and a typical step-pressure data chart.

the polyol/gas solution was calculated from CO_2 sorption amount and solution volume per unit mass of polyol (C). As a final step, this value was fed to the ADSA software to calculate (properly, by correcting gravitational forces with actual drop mass) the interfacial tension (D) [5,8].

A Teflon rod with a diameter of 2.03 mm was chosen as drop holder. The pendant drop was created by disposing a small amount of polyol on the top of the rod, using a pipette. Care was taken in order not to wet the lateral surface of the rod itself.

After having placed both the crucible containing the polyol and the rod with the polyol drop in the HT–HP view cell, sorption and ADSA experiments were carried out by isothermal pressure increments up to 6800 kPa, at 35 °C which is the typical temperature utilized in the industry to conduct polyurethane foam synthesis in presence of CO_2 at high pressure. In detail, sorption measurements were performed by step-wise increments of the gas pressure (500 kPa steps ca.), after the attainment of equilibrium sorption in the previous step. Concurrently, during each pressure step, image acquisition of the pendant drop was performed every 10 min.

Drop preparation is a fundamental step in ADSA technique, in particular in the selection of the drop size. It has been found that, if the drop is too small (Bond number $\ll 1$) and, correspondingly, its shape is close to a hemisphere, numerical problems arise in the fitting procedure; furthermore, if the drop is bigger than a critical volume (Bond number $\gg 1$), it necks and detaches from the rod [5,9,10]. Here, small or big depends on drop volume, drop mass, interfacial tension and density of outer phase (CO_2). Since all of these conditions change dramatically at the different CO_2 pressures, it is not possible, in the experimental range of interest in this work, to use a single drop size. As the CO_2 pressure increases, the drop swells until it detaches from the rod. In our case, we were interested in conditions of CO_2 at high pressure and we were, then, forced to use three different initial drop sizes (V_d^0 is the volume of the drop under vacuum), each suitable for a different pressure range. Fig. 4 reports the optical images of different drops for the different conditions of measure. The partial overlap of the pressure

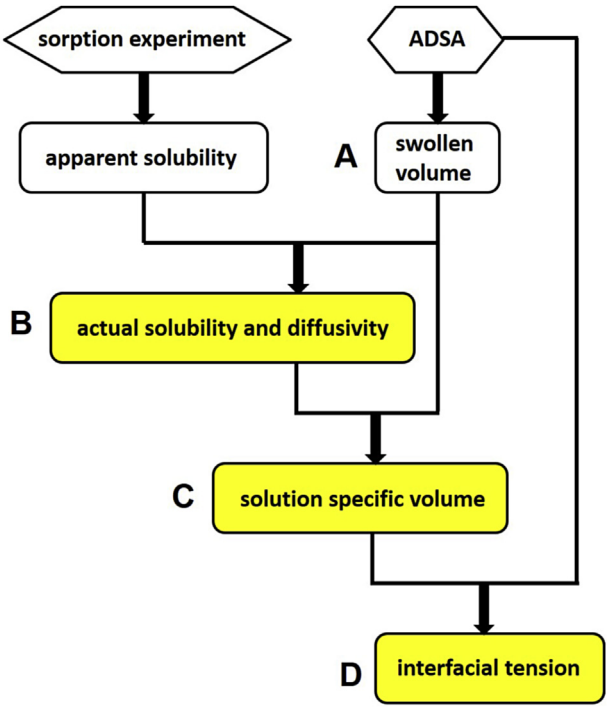

Fig. 3. Data flow used in the coupled sorption–ADSA measurement (in yellow properties measured in this contribution). (For interpretation of the references to colour in this figure legend, the reader is referred to the web version of this article.)

ranges (see Fig. 4) is then a good check for the reliability of the volume and interfacial tension data and for the whole data evaluation chain.

ADSA experiments were performed up to 6800 kPa, while gravimetric experiments were extended up to 8000 kPa. Gravimetric data were obtained on two replicates.

2.2. Materials

A formulated polyether polyol (Table 1) was supplied by DOW Italia S.r.l. (Correggio, RE, Italy) and used "as received". This polyol is the reference for the LIFE13-EN/IT/001238 project (http://ec.europa.eu/environment/life/). High purity grade CO_2 was supplied by SOL (Naples, Italy).

2.3. Data treatment

Data treatment is described in the following, according to the measurement flow chart reported in Fig. 3. Details of the whole data treatment chain are described in Pastore Carbone et al. [5].

2.3.1. Evaluation of the swelling of the polymer/gas solution

Firstly, the optical observation of volume changes of the polyol drop exposed to CO_2 atmosphere was used for the analysis of the swelling of the polyol/CO_2 solution. In particular, for each pressure step, the volume of the CO_2-saturated polyol drop, $V_d(p)$, was computed by integrating the drop profile, as performed by the ADSA software. The volume of the sample contained in the crucible, $V_c(p)$, at equilibrium, can then be calculated as by Eq. (1):

$$Vc(p) = \frac{V_d(p) - V_d^0}{V_d^0} V_c^0 + V_c^0 \quad (1)$$

where V_d^0 and V_c^0 are, respectively, the volume of the drop and the volume of the polyol contained in the crucible at initial conditions (under vacuum). It was assumed that, at equilibrium, drop curvature has negligible effects on specific volume and local gas concentration [11] and, consequently, that the drop and the sample in the crucible reach the same volume per unit mass of starting polyol.

2.3.2. Actual solubility and diffusivity

Data obtained from the gravimetric determination of mass transfer from the CO_2 phase to the polyol contained in a crucible suffer from buoyancy effect due to change in gas density at several pressures and to sample swelling upon sorption. The so-called "apparent solubility" needs to be corrected with the proper buoyancy force. Having calculated in Section 2.3.1. (A in Fig. 3), for each pressure, the volume at equilibrium of the sample contained in the crucible, $V_c(p)$, it was used for proper evaluation of buoyance, to correct gravimetric data thus giving the actual gas weight fraction in the polyol/CO_2 solution (ω_{ACT}), as calculated as by Eq. (2).

$$\omega_{ACT}(p) = \frac{W_{ACT}^{gas}(p)}{W_c^0 + W_{ACT}^{gas}(p)} \quad (2)$$

where W_c^0 is the initial weight of the sample contained in the crucible (as measured by an analytical balance) and W_{ACT}^{gas} is the actual gas weight gain, as calculated as by Eq. (3):

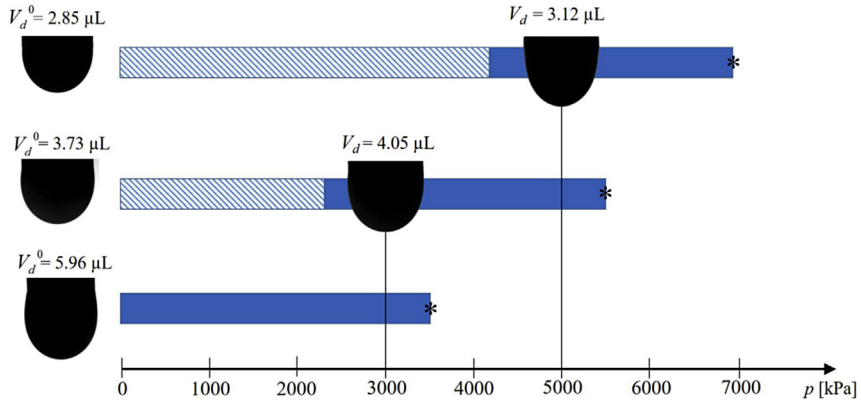

Fig. 4. Digitalized images of the different polyol drops utilized in the different pressure ranges (blue bar), under vacuum and at measuring pressure. Asterisk indicate drop detach event; dashed line indicate pressure range where numerical ADSA procedure gives inaccurate interfacial tension calculation. (For interpretation of the references to colour in this figure legend, the reader is referred to the web version of this article.)

Table 1
Composition of the "as received" polyether polyol.

Components	Molecular weight (Mw) (Da)	Parts (%)
Glycerin initiated polyether polyol	1000	
Amine initiated polyether polyol	500	95
Sorbitol initiated polyether polyol	700	
Sucrose/glycerin initiated polyether polyol	500	
Catalysts	/	3
Surfactant	/	2

$$W_{ACT}^{gas}(p) = BR_e - BR_e^0 + \rho_{gas}(p)[V_c(p) + V_h] \quad (3)$$

here, BR_e is the Rubotherm balance reading at equilibrium at each pressure (attainment of homogeneous CO_2 concentration), BR_e^0 is the initial balance reading at equilibrium (under vacuum), ρ_{gas} is the CO_2 density [12], V_h is the volume of crucible and of hook (see Fig. 1) that was previously determined by evaluating the buoyancy effect in a blank test with helium.

The kinetics of sample weight increase in step-wise sorption experiments was analyzed to gather information on the value of the average mutual diffusivity as a function of CO_2 concentration in the polyol. The average mutual diffusivity ($\overline{D}$) in each step-wise sorption experiment was calculated as follows [13]:

$$\overline{D} = \frac{\pi L^2}{4}\left(\frac{d(M_t/M_\infty)}{d(\sqrt{t})}\right)^2 \quad (4)$$

where M_t is the mass of the CO_2 sorbed at time t and M_∞ is the mass of the CO_2 sorbed at equilibrium and L is the actual sample thickness (sample is exposed to the gas phase on one side only). M_t has been calculated as $BR_{(t)} - BR_{(o)}$ and M_∞ has been calculated as $BR_{(\infty)} - BR_{(o)}$, where $BR_{(o)}$ is the balance reading just after the pressurization, $BR_{(t)}$ is the balance reading at time t, $BR_{(\infty)}$ is the balance reading at equilibrium.

The value of $\overline{D}$ calculated through Eq. (4) corresponds to the value of the CO_2 mutual diffusivity, $D(C)$ at an intermediate concentration, C, the value of which can be calculated according to the procedures proposed by Vrentas and Duda [14]. Since L increases as the CO_2 sorbed amount increases, the actual sample thickness used in this analysis was evaluated on the basis of the arithmetic average of initial and final measured equilibrium volume of the polymer-gas solution. It is worth noting that the evaluation of diffusivity was based on balance reading, and the buoyancy correction was applied only to correct for the initial lift promoted by the additive gas entering the measuring cell during the step pressure increase. Actually, the lift changes also during sorption due to the weight and, in turn, volume increase of the polyol-CO_2 mixture. However, in view of the slight weight increase during a step sorption, this correction was not applied.

2.3.3. Evaluation of specific volume of the polyol/CO_2 solution

Having determined gas sorption amount and solution volume per unit mass of polyol, these results were then used to calculate the specific volume of the polyol/gas solution. In detail, combining the volume (V_c) and the actual weight of the sample contained in the crucible (W_c) thus allowed for the calculation of the specific volume of the polyol/CO_2 solution, v_s, as by Eq. (5).

$$v_s(p) = \frac{V_c(p)}{W_c(p)} = \frac{V_c(p)}{\left(\frac{W_c^0}{1-\omega_{ACT}(p)}\right)} \quad (5)$$

2.3.4. Evaluation of interfacial tension of the polymer/gas solution

Finally, the determination of the interfacial tension of the separation surface between the polyol/CO_2 solution and the surrounding CO_2, γ, was performed by using the well-established ADSA, which consists in fitting the shape of the experimental drop (that was continuously monitored during the simultaneous measurement) to the theoretical drop profile according to the Laplace equation, properly modified to account for the action of the gravitational field [15–17]. Therefore, the specific volume of the solution at different pressures, $v_s(p)$, as determined according to Section 2.3.3. (C in Fig. 3), was used as input to the ADSA software to perform the calculation of the equilibrium value of interfacial tension at each pressure.

2.4. Gel permeation chromatography analysis

Gel Permeation Chromatography (GPC) analysis was conducted on the "as received" polyol and on the polyol recovered from the crucible after the sorption campaign (addressed to, in the following, as "treated" polyol) in order to verify any effect of the treatment on molecular weight.

The samples were completely dissolved in THF in concentration of ≈0.5% w/v and passed through a 0.22 μm PTFE membrane filter. Measurements were performed on an injected volume of 100 μL by using a Malvern – Viscotek GPC MAX/TDA 305 quadruple detector array equipped with a precolumn and two columns Phenogel Phenomenex with exclusion limits 106 and 103 respectively. The GPC instrument was used at flow rate of 0.8 mL/min and at column and system temperature of 35 °C. Universal calibration was based on a series of polystyrene standards ranging in molecular weight from 150000 to 1500.

2.5. Transmission Fourier transform infrared analysis

Fourier Transform Infrared (FT-IR) spectroscopy was conducted on the "as received" polyol and on the extracted fluid contained in the CO_2-rich phase spilled from the pressure vessel, after CO_2 volatilization (addressed to, in the following, as "extracted" polyol). Spectra were collected at room temperature by using a Nexus-Nicolet apparatus with a wavenumber resolution of 4 cm^{-1}, from 4000 to 400 cm^{-1}, for 64 scans.

3. Results and discussion

3.1. Sorption isotherm

Fig. 5 reports the sorption isotherm for the polyol/CO_2 solution (calculated as by eq. (2)), up to 8000 kPa and at a temperature of 35 °C, showing a rather linear dependence, with a maximum ω_{ACT} of 17% at a pressure of 8000 kPa. Data are also reported in Table 2.

Since polyol drop detaches at 6800 kPa (see Fig. 4), the last two data, at pressure of 7405 kPa and 7989 kPa, were estimated by extrapolating $V_d(p)$, as reported in the inset of Fig. 5.

It is worth of note, furthermore, that above 8000 kPa (at a

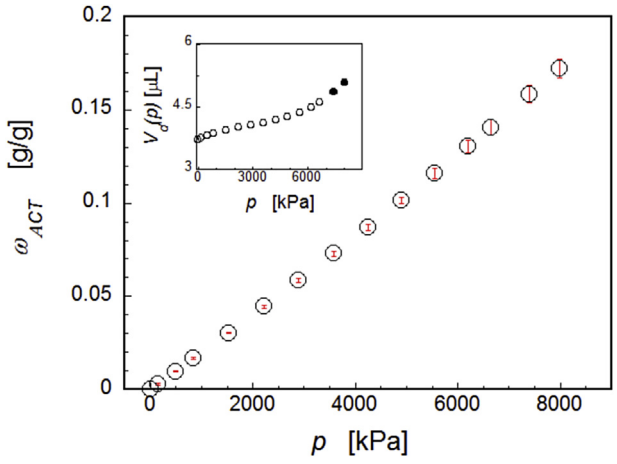

Fig. 5. Sorption isotherm of CO_2 in polyol at 35 °C (in red, the error bars). Inset: $V_d(p)$ vs. pressure. $V_d(p)$ data above 6800 kPa (closed symbols in the inset) have been extrapolated because of the occurrence of drop detachment event, to evaluate buoyancy corrected sorption data. (For interpretation of the references to colour in this figure legend, the reader is referred to the web version of this article.)

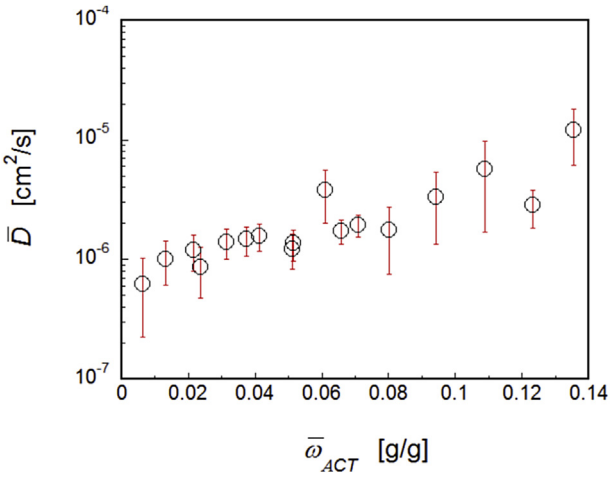

Fig. 6. Mutual diffusivity of CO_2 and polyol at 35 °C (in red, the error bars). (For interpretation of the references to colour in this figure legend, the reader is referred to the web version of this article.)

pressure of 8270 kPa) we observed a sharp reduction of the final equilibrium weight of the sample contained in the crucible (data not reported). This, as it will be described in the FT-IR section, was attributed to the partial solubilization of polyol in sc-CO_2 (extraction).

3.2. CO_2/polyol mutual diffusivity

The values of $\overline{D}$ for the polyol/CO_2 system, as obtained from Eq. (4), are reported in Fig. 6 and in Table 3, as a function of average CO_2 mass fraction ($\overline{\omega}_{ACT}$). Again, we made use of sample volume swelling to correct the initial sample thickness L through which sorption occurs and actual sample thickness used in this analysis was evaluated on the basis of the arithmetic average of initial and final measured equilibrium volume of the polyol/CO_2 solution. Within the investigated pressure range, it was found that $\overline{D}$ changes with CO_2 concentration, varying from 1e−6 to 1e−5 cm^2/s with CO_2 pressure changing from 0 to 6800 kPa. No other data on similar (polyol/CO_2) systems were found in the literature for proper comparison. As a general comment, measured polyol/CO_2 mutual diffusivities are rather low, with respect to typical molten polymer/penetrant systems utilized for foaming [8] and indicate that long residence times are needed in industrial applications to attain equilibrium.

3.3. Specific volume

Fig. 7 shows the specific volume of the polyol/CO_2 solutions in the investigated experimental range, calculated as by eq. (5). v_s data, reported in Table 4, evidence a non-monotonic dependence. In fact, when a polymer is exposed to a high-pressure gas, two mechanisms compete in affecting the specific volume: (i) compression of the gas-saturated polymer by the mechanical action of pressure exerted by the external gas; (ii) gas-solubilization. With the increase of external gas pressure, the latter mechanism is responsible for an increase of the volume, while the first is responsible for a reduction of the volume. In our case, $V_d(p)$ is monotonically increasing with gas pressure, proving a prevailing effect of the gas solubilization. However, mass increase of the gas saturated polymer drop is occurring. As a final balance, in our case, at low gas concentration, the mass increase is the dominant effect, and a reduction of v_s is observed. At higher gas concentration, conversely, the volume increase becomes the predominant effect. This non monotonic dependence has been already observed on

Table 2
CO_2 sorption at different pressure and at T = 35 °C.

p (kPa)	ω_{ACT} (g/g)	Uncertainty for $\omega_{ACT\ (g/g)}$
0	0	
153.1	0.0029	5e−04
500.0	0.0097	2e−04
845.4	0.0166	4e−04
1531.7	0.03041	2e−05
2215.9	0.0443	7e−04
2898.0	0.058	1e−03
3575.8	0.072	1e−03
4240.9	0.087	1e−03
4892.6	0.101	1e−03
5549.3	0.116	2e−03
6190.7	0.130	3e−03
6635.2	0.140	4e−03
7405.3	0.158	4e−03
7989.4	0.172	5e−03

Table 3
Mutual diffusivity at different average CO_2 mass fraction and at T = 35 °C.

$\overline{\omega}_{ACT}$ (g/g)	$\overline{D}$ (cm^2/s)
0.0064	6e−07
0.0132	1.0e−06
0.0216	1.1e−06
0.0235	8e−07
0.03147	1.4e−06
0.0374	1.5e−06
0.0414	1.6e−06
0.051	1.2e−06
0.052	1.3e−06
0.061	3.8e−06
0.066	1.7e−06
0.071	1.9e−06
0.080	1.7e−06
0.094	3.3e−06
0.109	5.7e−06
0.123	2.8e−06
0.135	1.21e−05

Uncertainty is ±5e−07 cm^2/s for $\overline{D}$.

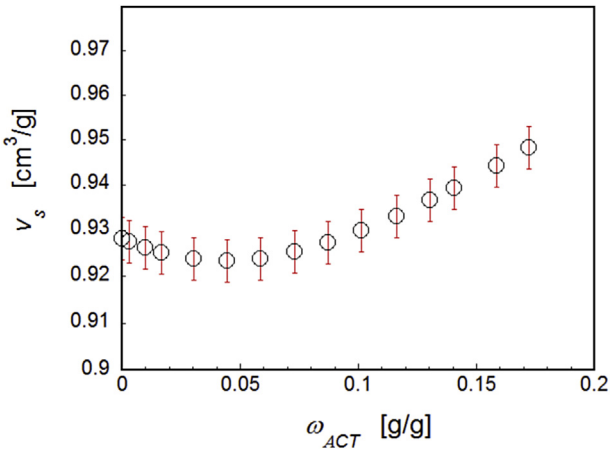

Fig. 7. Specific volume of polyol/CO_2 solutions at 35 °C (in red, the error bars). (For interpretation of the references to colour in this figure legend, the reader is referred to the web version of this article.)

PCL/CO_2 [5,8] and has been justified (and also verified by Raman spectroscopy) in view of the presence, in the PCL/CO_2 solution, of two populations of CO_2 molecules, one polymer-associated and one non-associated, with associated molecules contributing a lower volume of mixing as compared to non-associated ones and a prevalence of associated molecules at low CO_2 pressure [18]. As in the cited work, spectroscopic experiments on our system could reveal the existence of molecular interactions between the polyol and CO_2, which would help explaining the non-monotonic dependence of specific volume of polyol/CO_2 solution.

3.4. Interfacial tension of the polyol/gas solution

Fig. 8 reports the effect of CO_2 concentration on γ. In the selected experimental range, interfacial tension of the polyol was found to be nearly linear decreasing function of the CO_2 pressure (data are reported in Table 5). Such a decrease in the interfacial tension with the gas pressure has already been reported elsewhere [19–23] and is generally attributed to two concurrent phenomena [22,23]: (i) as pressure increases, the free energy density of CO_2 becomes closer to that of the polymer phase and the interfacial tension decreases; (ii) as gas pressure increases, the concentration of CO_2 in the polymer phase increases thus further promoting a decrease of interfacial tension since the two phases in contact become more similar.

Table 4
Specific volumes at different CO_2 mass fraction and at T = 35 °C.

ω_{ACT} (g/g)	v_s (cm^3/g)
0	0.928
0.0029	0.927
0.0097	0.926
0.0166	0.925
0.03041	0.924
0.0443	0.923
0.058	0.924
0.072	0.925
0.087	0.927
0.101	0.929
0.116	0.933
0.130	0.936
0.140	0.939
0.158	0.944
0.172	0.948

Uncertainty is ±0.5% for v_s.

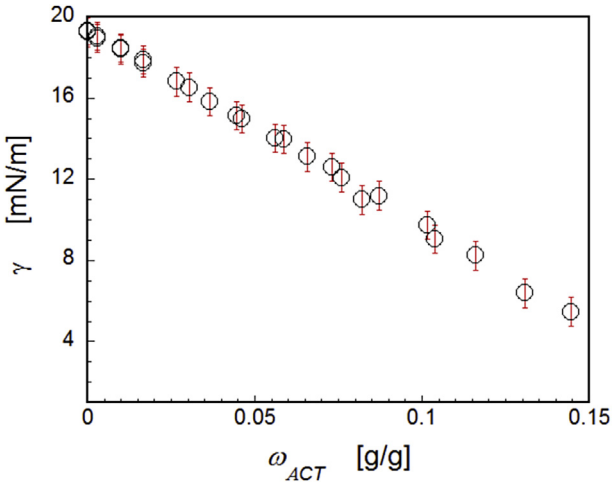

Fig. 8. Interfacial tension between polyol/CO_2 solutions and CO_2 at 35 °C (in red, the error bars). (For interpretation of the references to colour in this figure legend, the reader is referred to the web version of this article.)

Table 5
Interfacial tension at different CO_2 mass fraction and at T = 35 °C.

ω_{ACT} (g/g)	γ (mN/m)
0	19.3
0.0029	19.0
0.0097	18.4
0.0166	17.8
0.0265	16.8
0.03041	16.5
0.0364	15.8
0.0443	15.1
0.0462	14.9
0.056	14.0
0.058	13.9
0.065	13.1
0.072	12.5
0.075	12.0
0.087	11.1
0.082	10.9
0.101	9.7
0.103	9.0
0.116	8.2
0.130	6.3
0.144	5.4

Uncertainty is ±0.7 mN/m for γ.

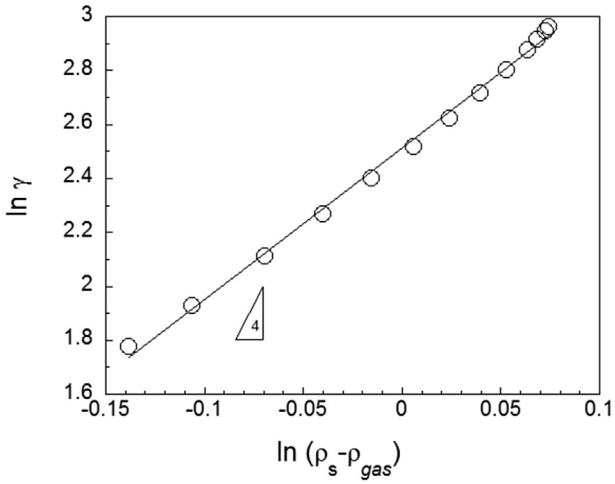

Fig. 9. Macleod plot for the polyol/CO2 solution (fitting with eq. (6)).

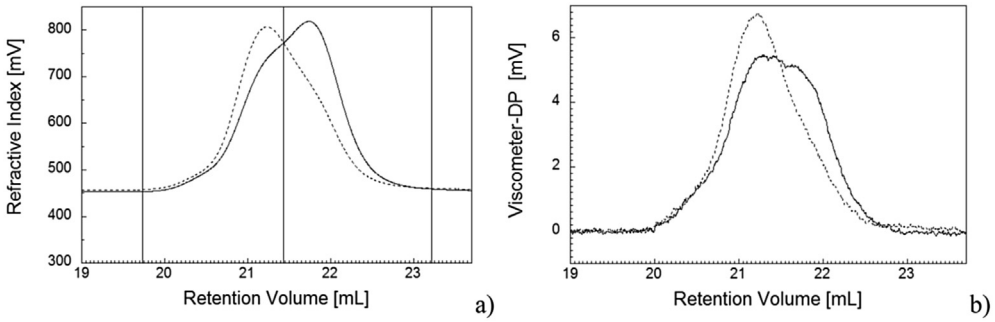

Fig. 10. GPC refractive index chromatograms (a) and GPC viscosity chromatograms (b) of "as received" polyol (solid line) and the "treated" polyol (dashed line).

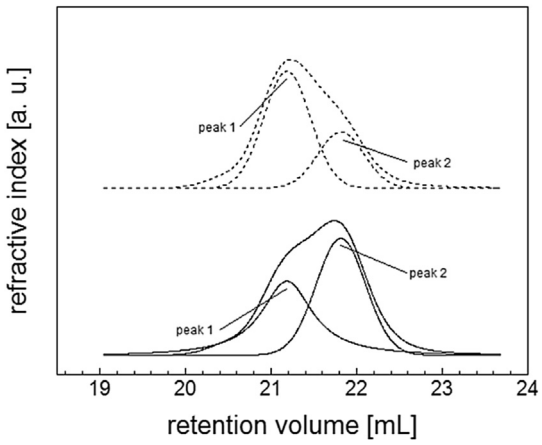

Fig. 11. GPC refractive index chromatograms of "as received" polyol (solid line) and the "treated" polyol (dashed line) fitted by two Gaussian functions.

It is important to note that at the highest CO_2 pressure of the investigated experimental range, these data reveal that the interfacial tension of the polyol/CO_2 solution is vanishing, which, by observing that the densities of the two phases are approaching, could justify the solubilization of the polyol in the CO_2-rich phase [24]. To verify this significant phenomenon, at the end of the coupled sorption-ADSA experimental campaign, when the pressure vessel was at highest pressure and we observed the sharp reduction of the weight of the polymer contained in the crucible, we both spilled out the CO_2-rich phase and the "treated" polyol for further characterization, as it is reported in the following.

A common treatment of interfacial tension data is based on Macleod's relation (eq. (6)), in which γ is reported as function of the density difference between the dense and the light phases (in our case the polyol/CO_2 solution and the CO_2, respectively):

$$\gamma = C\left(\rho_s - \rho_{gas}\right)^n \tag{6}$$

where C is a characteristic constant for a given liquid, $\rho_s = 1/v_s$ is the density of the polyol/CO_2 solution, and n is the Macleod's exponent. The exponent n is close to 4 for many unassociated liquids of low-molecular-weight substances [25]. In our case ln C is equal to 2.5 ($C = 12.2$) while n is equal to 5.8 (see Fig. 9).

According to Sugden's equation (eq. (7)) [26], from C it is possible to calculate the parachor (P), an empirical constant that relates γ to the molecular volume:

$$P = C^{1/n}M = \frac{M}{\rho_s - \rho_{gas}}\gamma^{1/n} \tag{7}$$

where M is the molecular weight of the liquid. The quantity $M/(\rho_s - \rho_{gas})$ has the dimensions of a volume and, at low temperatures, where ρ_{gas} becomes very small, is the molecular volume of the polyol. In our case, $Mw = 600$ and $n = 5.8$ giving $P = 925$ $(cm^3/mol)^*(mN/m)^{1/5.8}$ (use of $n = 4$ gives an estimate for $P = 1124$ $(cm^3/mol)^*(mN/m)^{1/4}$).

The values of γ can be also correlated to CO_2 concentration by using the following empirical equation [27]:

$$\gamma = (1 - \omega_{ACT})\gamma_{polyol}^{1/r} \tag{8}$$

where γ_{polyol} is the surface tension of the "as received" polyol at 0 kPa.

From the fitting of the experimental data (not shown), the parameter r was estimated to be equal to 0.979.

3.5. GPC characterization

In Fig. 10a and b, the GPC refractive index and viscosity chromatograms, for the "as received" and the "treated" polyol, are reported. Both detection responses revealed that the "treated" polyol is missing some lower molecular weight fraction with respect to the "as received" one, possibly proving the extraction by the CO_2 of the polyol contained in the crucible.

Data reveal the presence of two main molecular weight distributions, as also shown in Fig. 11 reporting the fitting of the refractive index chromatograms by two Gaussian functions (indicated as peak 1 and peak 2). For a quantitative estimation of the relative concentration of the "as received" and the "treated" polyol, Table 6 reports the variation of the relative composition, above and below 600 Da (corresponding to the formulated polyol Mw average), which can be explained assuming that 56% of the fraction below 600 Da is extracted by CO_2. To further verify this, FT-IR was conducted on the "as received" and the "extracted" polyols, as follows.

Table 6
Sample concentrations, average Mws and relative composition of "as received" and "treated" polyols.

	Sample concentration mg/mL	Average Mw peak 1	Average Mw peak 2	% above 600 Da (peak 1)	% below 600 Da (peak 1)
"as received" polyol	5.656	738	302	68.7	31.3
"treated" polyol	5.572	877	298	83.3	16.7

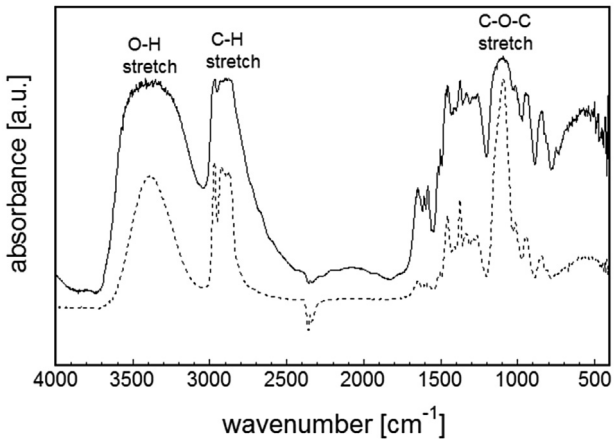

Fig. 12. FT-IR spectra of the "as received" polyol (solid line) and the "extracted" polyol (dashed line).

3.6. FT-IR characterization

Fig. 12 shows the FT-IR spectra of the "as received" polyol and of the "extracted" fluid contained in the CO_2-rich phase spilled from the pressure vessel, after CO_2 volatilization. It can be observed that curves present the same spectral features with the main characteristic absorption bands of a polyether polyol at 1100 cm^{-1} (C-O-C ether stretch), 2840 cm^{-1} (C-H stretch) and at 3100–3600 cm^{-1} (O-H stretch) [28,29]. This may confirm that part of polyol was solubilized in CO_2 at high pressures, thereby justifying the weight reduction observed at 8270 kPa.

4. Conclusions

Fully-experimental, coupled gravimetry-Axisymmetric Drop Shape Analysis has been utilized for measurement of solubility, diffusivity, specific volume and interfacial tension of polyol/CO_2 solutions, at 35 °C and at pressures up to 8000 kPa.

In the investigated experimental range, the sorption isotherm for the polyol/CO_2 solution shows a rather linear CO_2 pressure dependence, with a maximum ω_{ACT} of 17% at 8000 kPa. Mutual diffusivity goes from 1e−6 to 1e−5 cm^2/s in the whole experimental range, while the specific volume data evidence a non-monotonic dependence on CO_2 mass fraction. Furthermore interfacial tension of the polyol was found to be a nearly linear decreasing function of the CO_2 pressure. Finally, it has been found that, at pressures higher than 8000 kPa, low molecular weight components of polyol are solubilized in sc-CO_2, as confirmed by GPC and FT-IR analysis.

Acknowledgements

The authors are grateful to Mr. Stefano Marrazzo for the machining of the teflon rod and to Dr. Barbara Liguori (*Dipartimento di Ingegneria Chimica, dei Materiali e della Produzione Industriale, University of Naples Federico II*) for FT-IR analysis.

References

[1] D. Randall, S. Lee, The Polyurethanes Book, J. Wiley, New York, 2002.
[2] K.H. Choe, D.S. Lee, W.J. Seo, W.N. Kim, Properties of rigid polyurethane foams with blowing agents and catalysts, Polym. J. 36 (2004) 368–373.
[3] Occhiello, E.; Golini, P. Process for producing rigid polyurethane foams and finished articles obtained therefrom. U.S. Patent 20,040,092,616, May 13, 2004.
[4] E. Di Maio, G. Mensitieri, M.G. Pastore Carbone, G. Scherillo, in: S. Iannace, C.B. Park (Eds.), Biofoams: Science and Applications of Bio-based Cellular and Porous Materials, CRC Press, London, 2015, pp. 97–151.
[5] M.G. Pastore Carbone, E. Di Maio, E. Iannace, G. Mensitieri, Simultaneous experimental evaluation of solubility, diffusivity, interfacial tension and specific volume of polymer/gas solutions, Polym. Test. 30 (2011) 303–309.
[6] T. Guadagno, S.G. Kazarian, High-pressure CO_2-expanded solvents: simultaneous measurement of CO_2 sorption and swelling of liquid polymers with in-situ near-IR spectroscopy, J. Phys. Chem. B 108 (2004) 13995–13999.
[7] T. Fieback, W. Michaeli, S. Latz, M.E. Mondéjar, Sorption and Swelling Measurements of CO_2 and N_2 on polyol for their use as blowing agents in a new pu foaming process device, Ind. Eng. Chem. Res. 50 (2011) 7631–7636.
[8] M.G. Pastore Carbone, E. Di Maio, G. Scherillo, G. Mensitieri, S. Iannace, Solubility, mutual diffusivity, specific volume and interfacial tension of molten PCL/CO_2 solutions by a fully experimental procedure: effect of pressure and temperature, J. Supercrit. Fluids 67 (2012) 131–138.
[9] M. Hoorfar, A.W. Neumann, Recent progress in axisymmetric drop shape analysis (ADSA), Adv. Colloid Interface Sci. 121 (2006) 25–49.
[10] S.M.I. Saad, Z. Policova, E.J. Acosta, A.W. Neumann, Range of validity of drop shape techniques for surface tension measurement, Langmuir 26 (2010) 14004–14013.
[11] R.T. Dehoff, Thermodynamics in Materials Science, McGraw-Hill, New York, 1993, pp. 409–464.
[12] R. Span, W. Wagner, A new equation of state for carbon dioxide covering the fluid region from the triple-point temperature to 1100 K at pressures up to 800 MPa, J. Phys. Chem. Ref. Data 25 (1996) 1509–1596.
[13] J. Crank, The Mathematics of Diffusion, second ed., Oxford University Press, Oxford, 1975, pp. 47–64.
[14] J.S. Vrentas, J.L. Duda, Y.C. Ni, Analysis of step-change sorption experiments, J. Polym. Sci. Part B Polym. Phys. 15 (1977) 2039–2045.
[15] S. Bashforth, J.C. Adams, An Attempt to Test Capillary Action, Cambridge University Press and Deighton Pub, Bell and Co., London, 1882, pp. 13–56.
[16] O.I. del Rio, A.W. Neumann, Axisymmetric drop shape analysis: computational methods for the measurement of interfacial properties from the shape and dimensions of pendant and sessile drops, J. Colloid Interface Sci. 196 (1997) 136–147.
[17] P. Cheng, D. Li, L. Boruvka, Y. Rotenberg, A.W. Neumann, Automation of axisymmetric drop shape analysis for measurements of interfacial tensions and contact angles, Colloids Surf. 43 (1990) 151–167.
[18] M.G. Pastore Carbone, E. Di Maio, M. Pellegrino, A. Braeuer, G. Mensitieri, On the unexpected non-monotonic profile of specific volume observed in PCL/CO_2 solutions, Polymer 56 (2015) 252–255.
[19] S.P. Nalawade, F. Picchioni, L.P.B.M. Janssen, D.W. Grijpma, J. Feijen, Investigation of the interaction of CO_2 with poly(L-lactide), poly(DL-lactide) and poly(ε-caprolactone) using FTIR spectroscopy, J. Appl. Polym. Sci. 109 (2008) 3376–3381.
[20] D. Liu, D.L. Tomasko, Carbon dioxide sorption and dilation of poly(lactide-coglycolide), J. Supercrit. Fluids. 39 (2007) 416–425.
[21] H. Li, L.J. Lee, D.L. Tomasko, Effect of carbon dioxide on the interfacial tension of polymer melts, Ind. Eng. Chem. Res. 43 (2004) 509–514.
[22] K.L. Harrison, S.R.P. da Rocha, M.Z. Yates, K.P. Johnston, D. Canelas, J.M. De Simone, Interfacial activity of polymeric surfactants at the polystyrene–carbon dioxide interface, Langmuir 14 (1998) 6855–6863.
[23] K.L. Harrison, K.P. Johnston, I.C. Sanchez, Effect of surfactants on the interfacial tension between supercritical carbon dioxide and polyethylene glycol, Langmuir 12 (1996) 2637–2644.
[24] E. Kiran, J.F. Brennecke, Supercritical Fluid Engineering Science: Fundamentals and Applications; ACS Symposium Series 514, American Chemical Society, Washington, DC, 1993.
[25] D.B. Macleod, On a relation between surface tension and density, Trans. Faraday So. 19 (1923) 38–41.
[26] S. Sudgen, Relation between surface tension, density, and chemical composition, J. Chem. Soc. Trans. 125 (1924) 1177–1189.
[27] R. Reid, J.M. Prausnitz, B.E. Poling, The Properties of Gases and Liquids, fourth ed., McGraw-Hill International Editions, Singapore, 1988, pp. 656–732.
[28] G. Lligadas, J.C. Ronda, M. Galia', U. Biermann, J.O. Metzger, Synthesis and characterization of polyurethanes from epoxidized methyl oleate based polyether polyols as renewable resources, J. Polym. Sci. Part A Polym. Chem. 44 (2006) 634–645.
[29] P. Larkin, Infrared and Raman Spectroscopy, Principles and Spectral Interpretation, first ed., Elsevier, Oxford, 2011.